AGU PUBLICATIONS

JGR

Journal of Geophysical Research: Space Physics

RESEARCH ARTICLE
10.1002/2016JA023398

Key Points:
- Dayside magnetic reconnection location for northward IMF conditions
- Successful extension of the Maximum Magnetic shear model to predict the reconnection location for northward IMF
- Thirty percent of cusp events during northward IMF have signatures consistent with dayside reconnection locations

On the occurrence of magnetic reconnection equatorward of the cusps at the Earth's magnetopause during northward IMF conditions

K. J. Trattner[1], S. Thresher[1,2], L. Trenchi[3], S. A. Fuselier[4,5], S. M. Petrinec[6], W. K. Peterson[1], and M. F. Marcucci[7]

[1]Laboratory for Atmospheric and Space Physics, University of Colorado Boulder, Boulder, Colorado, USA, [2]Earth and Planetary Science Department, University of California, Santa Cruz, California, USA, [3]School of Physics & Astronomy, University of Southampton, Southampton, UK, [4]Southwest Research Institute, San Antonio, Texas, USA, [5]Physics and Astronomy Department, University of Texas at San Antonio, San Antonio, Texas, USA, [6]Lockheed-Martin ATC, Palo Alto, California, USA, [7]Istituto di Fisica dello Spazio Interplanetario, Rome, Italy

Correspondence to:
K. J. Trattner,
karlheinz.trattner@lasp.colorado.edu

Citation:
Trattner, K. J., S. Thresher, L. Trenchi, S. A. Fuselier, S. M. Petrinec, W. K. Peterson, and M. F. Marcucci (2017), On the occurrence of magnetic reconnection equatorward of the cusps at the Earth's magnetopause during northward IMF conditions, *J. Geophys. Res. Space Physics*, *122*, 605–617, doi:10.1002/2016JA023398.

Received 26 AUG 2016
Accepted 7 JAN 2017
Accepted article online 14 JAN 2017
Published online 24 JAN 2017

Abstract Magnetic reconnection changes the topology of magnetic field lines. This process is most readily observable with in situ instrumentation at the Earth's magnetopause as it creates open magnetic field lines to allow energy and momentum flux to flow from the solar wind to the magnetosphere. Most models use the direction of the interplanetary magnetic field (IMF) to determine the location of these magnetopause entry points, known as reconnection lines. Dayside locations of magnetic reconnection equatorward of the cusps are generally found during sustained intervals of southward IMF, while high-latitude region regions poleward of the cusps are observed for northward IMF conditions. In this study we discuss Double Star magnetopause crossings and a conjunction with a Polar cusp crossing during northward IMF conditions with a dominant IMF B_Y component. During all seven dayside magnetopause crossings, Double Star detected switching ion beams, a known signature for the presence of reconnection lines. In addition, Polar observed a cusp ion-energy dispersion profile typical for a dayside equatorial reconnection line. Using the cutoff velocities for the precipitating and mirrored ion beams in the cusp, the distance to the reconnection site is calculated, and this distance is traced back to the magnetopause, to the vicinity of the Double Star satellite locations. Our analysis shows that, for this case, the predicted line of maximum magnetic shear also coincides with that dayside reconnection location.

1. Introduction

Solar wind magnetic field lines draped around the Earth's geomagnetic field undergo a process called magnetic reconnection at the boundary between those two regimes known as the magnetopause. Magnetic reconnection is known to convert magnetic energy into kinetic energy and heat and is a fundamental process in many environments, spanning from laboratory plasmas to the heliosphere, the solar atmosphere, and to astrophysical phenomena.

Magnetic reconnection was originally proposed by *Dungey* [1961] as a process that allows the merging of geomagnetic and interplanetary magnetic field lines (IMF) of opposite polarity, in order to explain the circulation of magnetic flux and plasma in the outer magnetosphere and high-latitude ionosphere. This antiparallel reconnection scenario should occur at the subsolar magnetopause and near the equator during southward interplanetary magnetic field (IMF) conditions. For northward IMF conditions, the antiparallel reconnection scenario is known to occur at high latitudes poleward of the magnetospheric cusps [e.g., *Dungey,* 1963; *Crooker*, 1979; *Gosling et al.,* 1991]. However, the IMF usually exhibits a significant west-east component ($B_Y \neq 0$) for which the antiparallel reconnection model predicts a location split at local noon which results in two separate reconnection regions in the two opposite hemispheres [e.g., *Luhmann et al.,* 1984].

The component reconnection tilted X line model was proposed as an alternative to the antiparallel reconnection scenario [e.g., *Sonnerup,* 1974; *Gonzalez and Mozer*, 1974; *Cowley and Owen,* 1989; *Escoubet et al.,* 1992; *Moore et al.,* 2002]. For southward IMF conditions, the reconnection location for the component reconnection tilted X line model would be anchored at the subsolar point and extends continuously along the dayside magnetopause. The tilt of the reconnection line relative to the equatorial plane is determined by the ratio of the IMF east-west to north-south (B_Y/B_Z) components.

Evidence for magnetic reconnection at the Earth's magnetopause can be found in observations of accelerated D-shaped ion distributions within the dayside magnetopause boundary layer [e.g., *Cowley,* 1982; *Paschmann et al.,* 1979; *Gosling et al.,* 1982; *Pu et al.,* 2007; *Dunlop et al.,* 2009, 2011], from continuous magnetosheath plasma precipitation into the magnetospheric cusp regions [e.g., *Lockwood and Smith*, 1992; *Fuselier et al.,* 2000; *Trattner et al.,* 2002; *Escoubet et al.,* 2006, 2013] and in the ionosphere in the form of transient reconnection signatures [e.g., *Lockwood and Smith,* 1989, 1994]. These evidence has been documented for southward IMF conditions [e.g., *Sonnerup et al.,* 1981*; Fuselier et al.,* 1991; *Phan et al.,* 1996, 2000] as well as for northward IMF conditions [e.g., *Gosling et al.,* 1991; *Kessel et al.,* 1996; *Trattner et al.,* 2004]. Magnetic reconnection is also known to be a fundamentally multiscale process along the magnetopause surface [e.g., *Burch et al.,* 1982*; Escoubet et al.,* 1992*; Onsager et al.,* 2001], has been observed to be continuous [e.g., *Gosling et al.,* 1982*; Frey et al.,* 2003; *Phan et al.,* 2004], and tends to form long reconnection lines [e.g., *Fuselier et al.,* 2002; *Phan et al.,* 2006].

The reconnection site for northward IMF conditions is generally believed to be at high latitudes poleward of the cusp regions, where the merging magnetic fields are antiparallel. However, purely antiparallel conditions are not a necessary condition for reconnection to occur between magnetosheath and magnetospheric magnetic field lines, and shear angles as low as 50° have been observed [e.g., *Gosling et al.,* 1990]. In addition, some auroral emissions in the cusp region typically observed for southward IMF conditions, e.g., poleward moving auroral forms, are also observed during northward IMF conditions, consistent with a reconnection location equatorward of the cusps [*Oieroset et al.,* 1997; *Sandholt et al.*, 1998]. *Wing et al.* [2001] and *Escoubet et al.* [2007] observed double cusps originating from two separated sources at the magnetopause under dominant IMF B_Y and either IMF B_Z positive or negative. Observations in the high-altitude cusp during strongly northward IMF conditions also revealed D-shaped distributions typical for distributions observed at the subsolar magnetopause for a tilted component reconnection X line [*Onsager and Fuselier*, 1994; *Chandler et al.,* 1999; *Fuselier et al.,* 1997].

The subject of this study is an unexpected finding during the validation of the Maximum Magnetic Shear model [*Trattner et al.,* 2007] that predicts the location of the dayside reconnection location. For this investigation we used 33 magnetopause crossings observed by the Double Star TC1 satellite equatorward of the cusps and previously analyzed by *Trenchi et al.* [2008, 2009]. These magnetopause crossings showed reversals of accelerated ion beams which indicates that the reconnection line is close and therefore providing a definitive location for the dayside reconnection line to be compared with the predictions of the Maximum Magnetic Shear model. Seven of the 33 events occurred during northward IMF conditions. The Maximum Magnetic Shear model was developed with events observed during southward IMF conditions, assuming that northward IMF conditions will cause reconnection locations poleward of the cusp where merging fields are antiparallel. However, the model in general determines the line of maximum magnetic shear across the dayside magnetopause for any IMF condition. This study revealed that the confirmed dayside reconnection locations for seven northward IMF events observed by Double Star TC1 also fit the predictions of the Maximum Magnetic Shear model. In addition, one of these TC1 magnetopause crossings had a conjunction with the Polar satellite in the southern cusp region for which we could use the low-velocity cutoff method and independently determine the dayside reconnection region where the cusp ions crossed the magnetopause. All three methodologies (direct observations, model predictions, and remote field line tracing) are consistent with the existence of a reconnection location in the subsolar region, as might be expected from a tilted component reconnection X line. Five of the events are discussed below. Two of the events occurred during strong IMF B_X conditions, and while these events are also consistent with the predicted dayside reconnection location, the IMF draping model configuration is much more sensitive under conditions of strong IMF B_X and is more challenging to objectively compare with observations.

2. Data Selection, Instrumentation, and Methodology

The seven magnetopause crossings used in this study have been observed by the Double Star TC1 satellite in an almost equatorial orbit with an apogee of 12.4 R_E [*Liu et al.,* 2005]. The plasma data used to identify these magnetopause crossings were observed by the Hot Ion Analyzer (HIA) [*Reme et al.,* 2005] and have also been used in a large magnetopause study by *Trenchi et al.* [2008]. The HIA instrument is a top-hat analyzer that covers the energy range from 5 eV/e to 32 keV/e and provides three-dimensional ion distribution functions

with a time resolution of 4 s. These distribution functions are used to calculate the plasma moments on board Double Star TC1. Magnetic field data, averaged down to 4 s resolution, are observed by the fluxgate magnetometer [*Carr et al.,* 2005]. To identify the magnetic reconnection events, *Trenchi et al.* [2008] use the Walén relation in the spacecraft reference frame. Details about the data set and methodology can be found in *Trenchi et al.* [2008, 2009].

The ion observations in the Southern Hemisphere cusp region were obtained by the Toroidal Imaging Mass-Angle Spectrograph (TIMAS) [*Shelley et al.,* 1995] on board the Polar spacecraft. The Polar spacecraft was launched into a nearly 90° inclination orbit on 24 February 1996, with a perigee and apogee of about 2 and 9 R_E, respectively. Using 28 energy steps, the Polar/TIMAS proton measurements cover the energy range from 15 eV/e to 33 keV/e during a 6 s spin period. The cusp ion distributions are generally observed at geocentric distances between 3.5 and 9 R_E.

Solar wind observations to calculate the magnetic shear at the magnetopause are provided by the Wind Solar Wind Experiment (SWE) [*Ogilvie et al.,* 1995], the Wind Magnetic Field Investigation (MFI) [*Lepping et al.,* 1995], the ACE Solar Wind Experiment (SWE) [*McComas et al.,* 1998], and the ACE Magnetic Field Instrument (MFI) [*Smith et al.,* 1998]. All solar wind and IMF data are available at CDAWeb.

The procedure to determine the local distance of the observing satellite to the reconnection site at the magnetopause was originally used by *Onsager et al.* [1990, 1991] in the Earth's plasma sheet boundary layer and is generally known as the low-velocity cutoff method. The methodology can also be applied to observations by satellites crossing the cusp region where the time-of-flight characteristics of precipitating and mirrored cusp ions are used. The distance X_r to the magnetopause reconnection site can be estimated by using the observed low-velocity cutoff velocities for the precipitating and mirrored ion distributions in combination with a magnetic field model to determine the distance between the cusp satellite and the ionospheric mirror point and is defined by the following:

$$X_r / X_m = 2\, V_e / (V_m - V_e) \tag{1}$$

where X_m is the distance to the ionospheric mirror point, V_e is the cutoff velocity of the precipitating (earthward propagating) ions, and V_m is the cutoff velocity of the mirrored distribution [e.g., *Onsager et al.,* 1990; *Fuselier et al.,* 2000]. The T96 model [*Tsyganenko*, 1995] is used to determine and trace the distances X_m and X_r along geomagnetic field lines, beginning at the cusp location of the Polar satellite, to either the ionospheric mirror point or the magnetopause reconnection location, respectively. This methodology led to the development of the Maximum Magnetic Shear model that predicts the location of the dayside magnetopause reconnection site as a function of the IMF conditions and was successfully applied in several cusp studies [e.g., *Fuselier et al.,* 2000; *Trattner et al.,* 2007, 2012].

3. Observations

Confirmed reconnection locations based on the observation of switching ion beams in the magnetosheath boundary layer by the Double Star TC1 satellite are compared with the predicted reconnection location by the Maximum Magnetic Shear model. Figure 1 shows magnetopause shear angle plots as seen from the Sun for four Double Star TC1 magnetopause crossings during northward IMF conditions on 4 April 2004 (top left), 25 March 2004 (top right), 2 March 2004 (bottom left), and 14 February 2005 (bottom right). The IMF clock angles for these events range from 54° to 84°. Thus, while all events occurred during northward IMF (clock angle $< 90°$) conditions, all events also had a dominant IMF B_Y component.

The color-coded magnetopause shear angle in each of the panels of Figure 1 is calculated with the T96 geomagnetic field directions together with the fully draped IMF (provided either by the ACE or Wind satellites) at the magnetopause for 10 min time intervals around the time of the Double Star TC1 magnetopause crossings. The magnetopause boundary for the internal or magnetospheric magnetic field uses the *Sibeck et al.* [1991] magnetopause fit which is part of the T96 model and axially symmetric. The external or magnetosheath magnetic field is represented by the *Cooling et al.* [2001] model which is based on the more general *Kobel and Flückiger* [1994] model.

The terminator plane ($X_{GSM} = 0$) at the magnetopause is depicted by a black circle in Figure 1. Magnetopause regions where the internal geomagnetic field and the external fully draped IMF are in a high shear

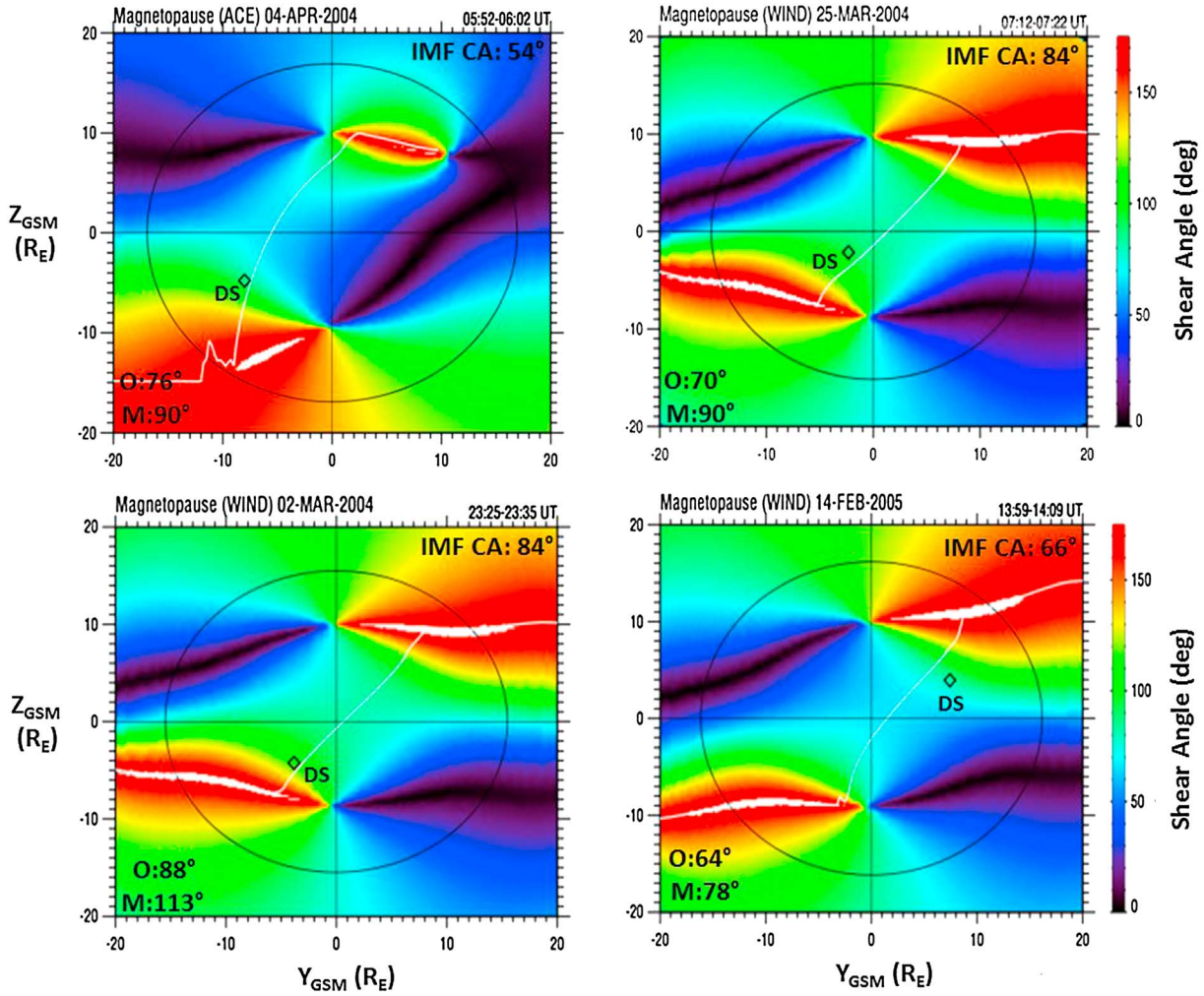

Figure 1. The magnetopause shear angle, as seen from the Sun, during four Double Star TC1 (DS) magnetopause crossings. The magnetopause shear angle was calculated using the magnetic field direction of the T96 model [*Tsyganenko*, 1995] combined with the fully draped IMF conditions at the magnetopause [*Kobel and Flückiger*, 1994] observed during the Double Star TC1 magnetopause crossings. White regions represent areas where the shear angle is within 3° of antiparallel. The black circle represents the magnetopause shape at the terminator plane. The white line crossing the dayside magnetopause represents the predicted reconnection location from the Maximum Magnetic Shear model [e.g., *Trattner et al.,* 2007] for the respective solar wind and IMF conditions during the magnetopause crossings. Also indicated are the positions of the TC1 satellite (black diamond symbols) and the observed (*O*) and model (*M*) magnetic shear angles at the positions of the satellite.

configuration (with shear angles ranging from 150° to 180°) are color coded in red, while regions with parallel magnetic fields are black. Areas where the magnetopause fields are within 3° of being exactly antiparallel are depicted as white regions within the nearly antiparallel red regions.

The black diamond symbols shown in the panels of Figure 1 represent the positions of the Double Star TC1 (DS) satellite during the respective magnetopause crossings at the reconnection location (switching ion beams in the magnetopause boundary layers). The white lines shown in Figure 1, crossing the dayside magnetopause to connect the antiparallel magnetic shear regions located at high latitudes, represent the line of maximum magnetic shear. This line was identified as the most likely location of the reconnection region by the Maximum Magnetic Shear model [e.g., *Trattner et al.,* 2007]. While this model was developed and validated only for southward IMF conditions, the procedure can also be used to determine the maximum magnetic shear lines during northward IMF conditions. For all seven northward IMF events considered in this study, with four of those events shown in Figure 1, the predicted maximum magnetic shear lines agree with the confirmed reconnection locations provided by the Double Star TC1 satellite.

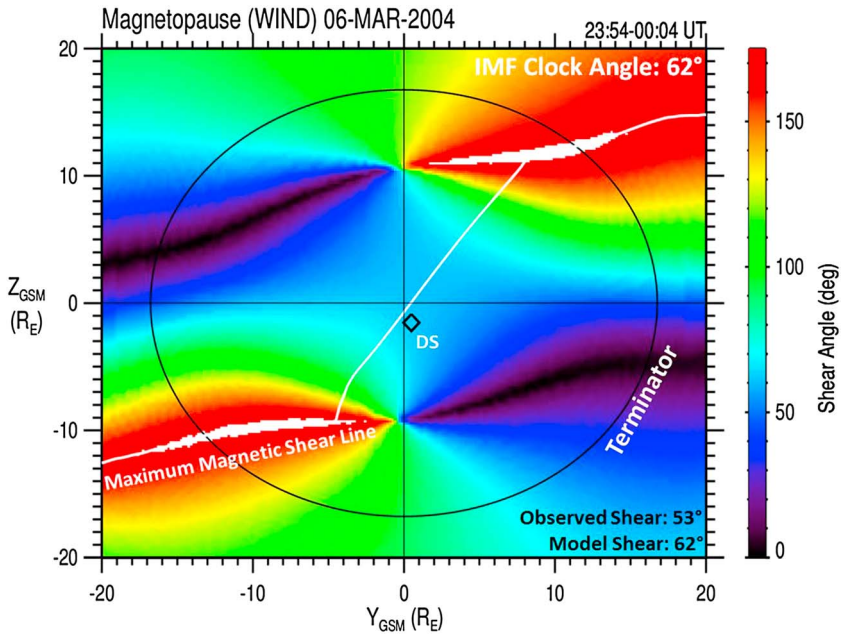

Figure 2. The magnetopause shear angle plot including the predicted reconnection line from the Maximum Magnetic Shear model (white line) and the position of the Double Star TC1 satellite (diamond symbol) during its 6 March 2004 magnetopause crossing.

The original study by *Trenchi et al.* [2008, 2009] contains, in addition to the 33 magnetopause events with switching accelerated ion beams within the magnetosheath boundary layer, another 110 magnetopause crossings which showed only single direction ion beams. Considering these two data bases, the Maximum Magnetic Shear model predicts the location of the reconnection site, or the direction to the reconnection location for the single beam events, correctly in 84% of all cases. A similar study by *Petrinec et al.* [2016] compared the locations and directions of accelerated ion beams at the magnetopause observed by the recently launched Magnetospheric Multiscale (MMS) satellites [e.g., *Burch et al.,* 2016] with predictions from the Maximum Magnetic Shear model and found an 88% agreement. Another recent study about ion beam acceleration as a function of the local magnetic shear angle using Cluster magnetopause crossings also used predictions from the Maximum Magnetic Shear model and reported a 74% agreement [*Vines et al.,* 2015]. It should be noted that of the events that failed the prediction, 72% shared a very specific parameter range. These events occurred around equinox and for an IMF clock angle of about 240°. The reason for this remarkable grouping is currently unknown and will be investigated in a subsequent study. However, these results show that the maximum shear model can be extended to northward IMF conditions (with dominant B_Y) without loss of statistical accuracy.

Figure 1 also reports the observed magnetopause shear angle at the location of Double Star TC1 satellite (*O*) and the model magnetic shear angle from the maximum shear calculation (*M*). This study provides the first comparison between the observed and derived magnetic shear at the magnetopause reconnection site to determine how accurate the IMF draping model represents draping about the actual magnetopause. The study revealed that the average error between the observed to the model magnetopause shear angle for the events in the Double Star data base was just $13° \pm 3.1°$.

Figure 2 shows the magnetopause shear angle plot for a fifth northward IMF event from the Double Star TC1 magnetopause crossings. The magnetopause crossing on 6 March 2004 from 23:54 UT to 00:04 UT occurred during an IMF clock angle of 62°. The prediction model draws a line of maximum magnetic shear across the dayside magnetopause close to the subsolar region (white line in Figure 2). The subsolar region is also the location of the Double Star TC1 satellite (DS) as it crossed the magnetopause and observed a switching ion beam in the boundary layer. The observed magnetopause shear angle at Double Star TC1 location was 53°, in good agreement with the model magnetopause shear angle of 62°. This event will be discussed in more

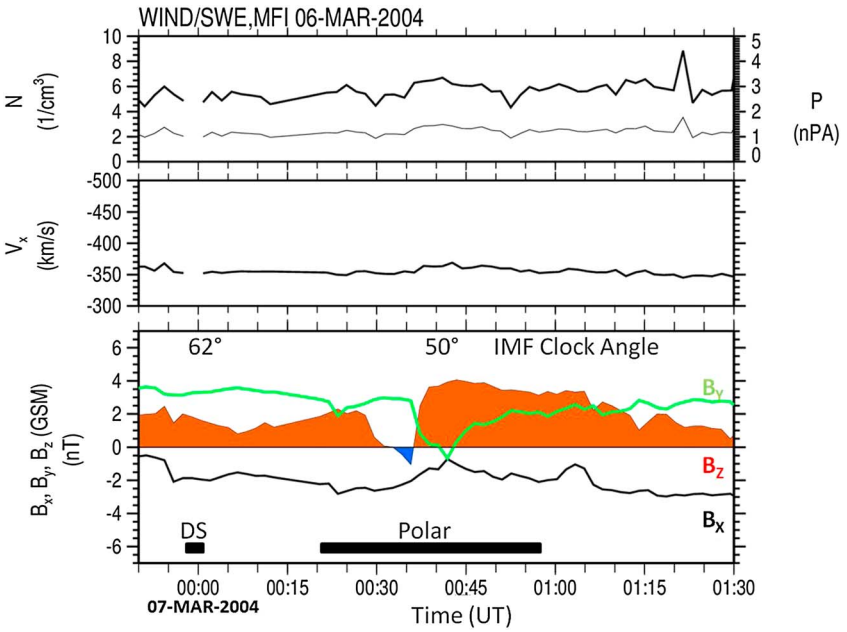

Figure 3. The solar wind density (top) *N*, (middle) solar wind velocity *V*, and the (bottom) IMF conditions for B_X (black line), B_Y (green line), and B_Z (red and blue filled area) during the Double Star TC1 (DS) magnetopause crossing and the Polar cusp crossing. The data are provided by the Wind SWE [*Ogilvie et al.,* 1995] and MFI [*Lepping et al.,* 1995] experiments and are convected to the magnetopause by about 13 min.

detail below and compared with observations from the Polar satellite which crossed the southern cusp region 20 min after the Double Star TC1 magnetopause crossing.

The solar wind conditions for 6 March 2004, from 23:50 UT to 01:30 UT on 7 March are shown in Figure 3. The data were observed by the Wind/SWE [*Ogilvie et al.,* 1995] and Wind/MFI [*Lepping et al.,* 1995] experiments located at about (46.1, 27.5, and −6.6) R_E for (*X*, *Y*, and *Z*) (GSM), respectively. To account for the travel time between the Wind satellite and the Earth's magnetopause, the data have been convected by about 13 min. Figure 3 (top) shows the solar wind density, *N*, for this cusp event with an average of about 5.6 cm^{-3} (thick black line). Also shown in this panel is the dynamic pressure, *P*, with an average of about 1.2 nPa (thin black line). Figure 3 (middle) shows the solar wind velocity, *V*, with an average of about 355.7 km/s. Figure 3 (bottom) shows the IMF components in GSM coordinates. The IMF is relatively stable throughout the time period with (−2, 2.4, and 2.1) (nT) for B_X (black line), B_Y (green line), and B_Z (red and blue colored areas), respectively. Black bars in Figure 3 (bottom) mark the times when Double Star TC1 crossed the magnetopause and when the Polar satellite observed the southern cusp region. During the Polar cusp crossing the IMF exhibits a brief southward turning and an equally brief period of negative IMF B_Y which have only a small influence on the average IMF conditions. The IMF clock angle, which is the basis for the magnetopause shear angle calculation, changes from 62° to 50° (see magnetopause shear angle plots shown in Figures 2 and 7) which also changes the model magnetic shear at the location of the Double Star TC1 satellite to 50.6°, in very good agreement with the observed magnetopause shear angle of 53°.

Figure 4 shows typical examples of cusp crossings by the Polar satellite during southward (top) and northward (bottom) IMF conditions. Plotted are H^+ omnidirectional flux measurements (1/(cm^2 s sr keV/e)) observed by the TIMAS instrument on board the Polar satellite for the respective crossings on 31 March 1996 and 8 October 1996. The dispersion features for these two cases are significantly different, which allows for an immediate determination of the magnetopause region where reconnection occurred.

The cusp crossing during southward IMF conditions on 31 March 1996 is characterized by a clear dispersion signature as Polar progresses to higher latitudes. For such conditions, newly opened field lines are convected poleward under the joint action of magnetic tension and shocked solar wind flow, causing lower energy particles to arrive at successively higher latitudes [e.g., *Rosenbauer et al*., 1975; *Shelley et al*., 1976]. The single and

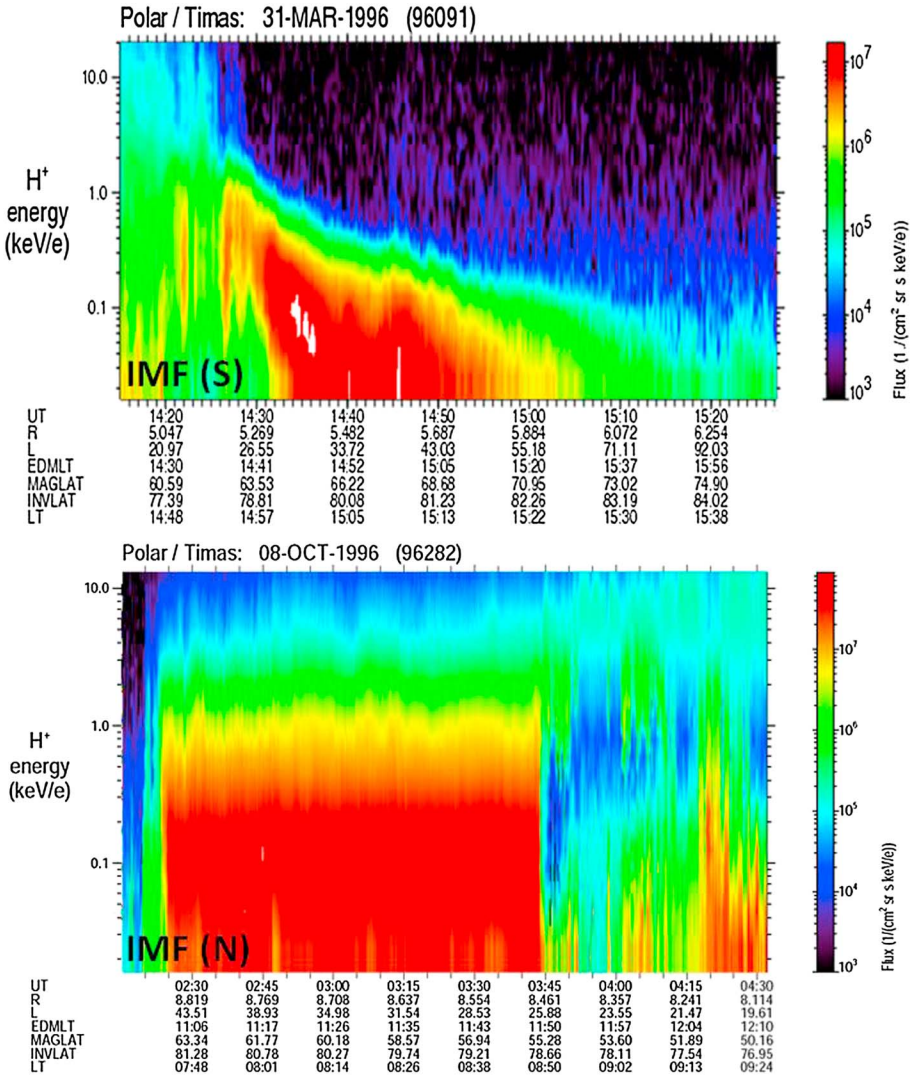

Figure 4. H^+ omnidirectional flux measurements (1/(cm^2 s sr keV/e)) observed by the TIMAS instrument on board the Polar satellite for two cusp crossings on 31 March 1996 and 8 October 1996 during southward and northward IMF conditions, respectively. The cusp crossings are characterized by a clear dispersion signature during southward IMF conditions, typical for an equatorward reconnection location, and a more box-like shape for northward IMF conditions, typical for a reconnection location poleward of the cusp.

continuous dispersion in the ions is also an indication for a steady rate of reconnection at the magnetopause. More commonly, the reconnection rate would vary, causing a discontinuous ion precipitation with invariant latitude which results in flux variations and sudden changes, or "steps," in the cusp ion dispersion signature [e.g., *Newell and Meng,* 1991; *Escoubet et al.,* 1992; *Lockwood and Smith*, 1992].

In contrast, cusp crossings during northward IMF conditions exhibit a more box-like shape with only a weak reverse dispersion feature indicating reconnection between magnetosheath field lines and high-latitude field lines poleward of the Earth's cusps [e.g., *Gosling et al.,* 1991; *Phan et al.,* 2003; *Trattner et al.,* 2004; *Lavraud et al.,* 2005]. These reconnected field lines convect slowly sunward against the magnetosheath convection flow allowing for ions of all energies to arrive at the observing satellite [e.g., *Escoubet et al.,* 2008]. A detailed review of the appearance of cusp structures during changing IMF conditions can be found in *Pitout et al*. [2009].

Figure 5 shows the Southern Hemisphere Polar cusp crossing on 7 March 2004 just after the Double Star TC1 satellite crossed the magnetopause. At that point of the mission, the TIMAS instrument suffered from

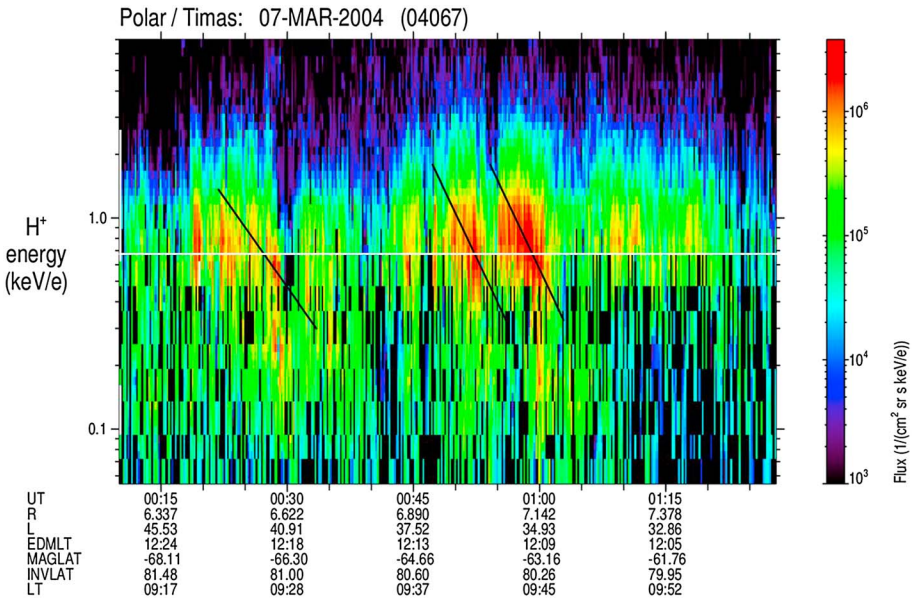

Figure 5. H^+ omnidirectional flux measurements (1/(cm^2 s sr keV/e)) observed by the TIMAS instrument on board the Polar satellite during the cusp crossings on 7 March 2004 shortly after the Double Star TC1 magnetopause crossing. This southern cusp crossing shows several distinct dispersion signatures, marked by black lines, as expected for an equatorward reconnection location.

decreased sensitivity in the lower energy channels. However, the flux observations around and above 700 eV were not affected by the change in sensitivity (thin white line in Figure 5). Plotted again are the H^+ omnidirectional flux measurements (1/(cm^2 s sr keV/e)) between 00:10 UT and 01:30 UT. Within that time interval three step-up ion dispersion signatures are observed and marked with black lines. These dispersions are in agreement with step-up cusp structures that represent discrete reconnection pulses at the magnetopause reconnection line and indicators for an equatorward reconnection line. This scenario is described in the pulsating cusp model [e.g., *Cowley et al.,* 1991; *Smith and Lockwood*, 1990]. In the next paragraph we use the ion dispersions shown in Figure 5 together with the low-velocity cutoff method described above to determine the location of the reconnection site [e.g., *Trattner et al.,* 2007].

Figure 6 (top) shows the distance to the reconnection line versus UT for the Polar/TIMAS distributions observed during the 7 March 2004 cusp crossing. Uncertainties in the distance calculations are defined as one half the difference between the distributions peak velocity and the low-velocity cutoff [e.g., *Fuselier et al.,* 2000]. The distance to the reconnection site from the Polar satellite in the southern cusp to the magnetopause shows some variation over a range from about 7 to 18 R_E. The range of these distance calculations can be explained with the north-south location of the reconnection line across the magnetopause (as shown in Figures 2 and 7) and the motion of the Polar satellite in magnetic local time (from 12:22 to 12:07 eccentric dipole magnetic local time shown in Figure 5).

Figure 6 (bottom) shows the magnetopause as seen from the dawn sector (left) and from the Sun (right). As with the magnetic shear angle plots above, the circle in Figure 6 (bottom right) represents the size of the magnetopause at the $X = 0$ terminator plane, separating the dayside magnetopause inside the circle from the tail side magnetopause outside the circle. Emanating from the position of the Polar satellite in the southern cusp during the 7 March 2004 event, thin green and blue lines represent two geomagnetic field lines from the T96 model. The diamond symbols in Figure 6 show the location of the reconnection points at the magnetopause which are derived from tracing the calculated distance in the top panel along those T96 magnetic field lines back to the magnetopause.

Figure 7 combines the prediction of the reconnection location from the maximum magnetic shear line (white line) with the field line trace points from the Polar cusp crossing (black square symbols) and the location of the Double Star TC1 satellite as it crossed the magnetopause and observed a switching ion beam (green

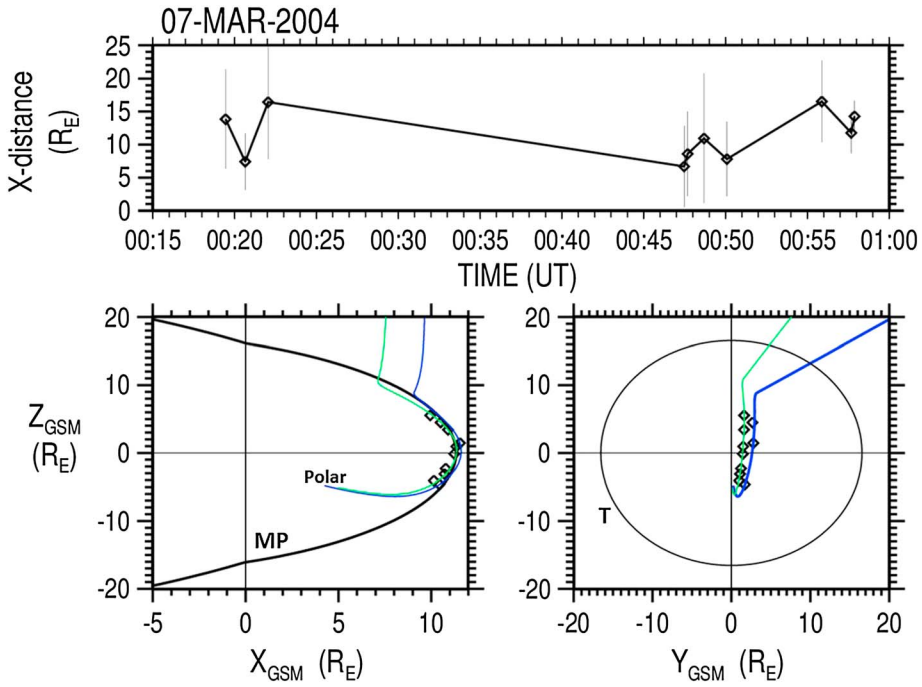

Figure 6. The (top) distance to the reconnection site for the Polar Southern Hemisphere cusp crossing on 7 March 2004 and the location of the reconnection site at the magnetopause, marked by black diamonds, as seen from (bottom left) dawn and from the (bottom right) Sun. The distances are traced along geomagnetic field lines (green and blue lines) from the T96 magnetic field model starting at the position of the Polar spacecraft in the southern cusp toward the magnetopause. The circle in Figure 6 (bottom right) represents the location of the magnetopause at the terminator plane, separating the dayside magnetopause (inside the circle) from the nightside magnetopause (outside the circle).

diamond symbol). Plotted is the magnetopause shear angle during the Polar cusp crossing on 7 March 2016, as seen from the Sun. The layout is the same as in Figure 2. The maximum magnetic shear line for these northward IMF conditions with an IMF clock angle of 50° crosses the subsolar region and is in perfect agreement with the location of the switching ion beam observed by Double Star TC1 [*Trenchi et al.,* 2008]. This confirmed location of a dayside reconnection line is also in agreement with the field line trace points derived from the Polar cusp crossing which straddle the predicted reconnection location across the dayside. The steep north-south slope of the reconnection location over a limited range in local time explains the large variation of the distance calculation as discussed in Figure 6.

In the example shown in Figure 7, the line of maximum magnetic shear crosses the dayside magnetopause close to the subsolar region surrounded by a large area with very similar magnetic shear conditions. A recent study by *Petrinec et al*. [2014] showed that the area several Earth radii away from the line of maximum magnetic shear is often only 2° to 3° from the local maximum value. Despite these small and almost insignificant changes in magnetic shear, the trace points derived from ion observations in the cusps [e.g., *Trattner et al.,* 2007] as well as in situ observations of reconnection lines at the magnetopause [e.g., *Dunlop et al.,* 2011; *Trattner et al.,* 2012, 2016; *Petrinec et al.,* 2016] have consistently clustered around the line of maximum magnetic shear.

The Polar cusp data base used to investigate the location of the magnetopause reconnection line, which led to the development of the Maximum Magnetic Shear model, contains 1328 cusp crossings over a time period from March 1996 to December 1998. About 270 of those events occurred during northward IMF conditions. For these events we expect to find a cusp dispersion resembling the dispersion shown in Figure 4 (bottom) above. However, a significant number of cusp crossings show typical step-up dispersion signatures with multiple magnetopause injection events, consistent with a dayside reconnection location. A survey of all 270 cusp crossings for northward IMF indicates that these dispersions are observed for about 29% of the events.

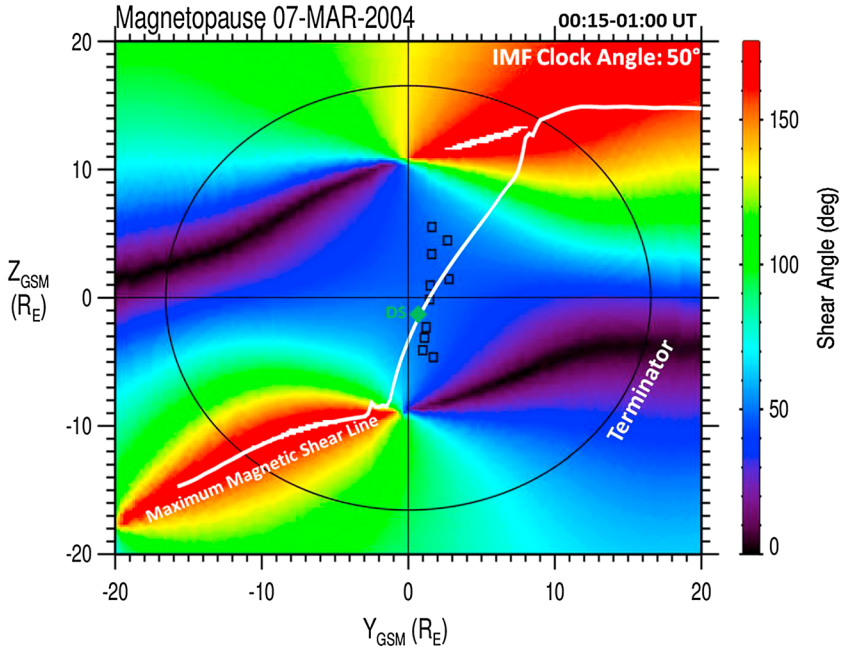

Figure 7. The magnetopause shear angle plot for the Polar cusp crossing on 7 March 2004. Overlaid are the predicted reconnection line from the Maximum Magnetic Shear model (white line), the position of the Double Star TC1 satellite (green diamond) and the field line trace points from the Polar/TIMAS Southern Hemisphere cusp crossing (black squares).

4. Summary and Conclusions

This study describes events with stable dayside reconnection locations for northward IMF conditions. Such conditions are thought to cause reconnection to occur at high latitudes poleward of the cusps as shown in the original study by *Dungey* [1963] and subsequent discussion of antiparallel reconnection in many studies [e.g., *Fuselier et al.,* 2000; *Frey et al.,* 2003; *Fuselier et al.,* 2003; *Trattner et al.,* 2004]. However, observations of auroral emissions and D-shaped distributions typical for reconnection locations at the subsolar magnetopause have also been reported [e.g., *Onsager and Fuselier*, 1994; *Fuselier et al.,* 1997; *Oieroset et al.,* 1997]. A recent study by *Trattner et al.* [2016], using magnetopause observations by MMS, showed that dayside reconnection lines exposed to a sudden northward turning of the IMF remained on the dayside and exhibit a several minutes long delay to adjust to the new conditions [*Trattner et al.,* 2016]. On the other hand, the northward IMF conditions imply the presence of an intense guide field (the field component along the X line orientation) that could be responsible for a motion of the X line along the magnetopause due to the diamagnetic drift effect [*Trenchi et al.,* 2015].

In this study we used a magnetopause data base from the Double Star mission. The data base was assembled and used in a study by *Trenchi et al.* [2008, 2009] where they investigated the ion beams in the boundary layers to determine the direction of the magnetopause reconnection location relative to the observing satellite. Of special interest is a subset of the data base with 33 events for which the ion beams switched direction, while Double Star TC1 crossed the magnetopause, a well-documented signature for a satellite located at the reconnection site [e.g., *Phan et al.,* 2003; *Trattner et al.,* 2012].

The Maximum Magnetic Shear model to predict the dayside location of the reconnection site was developed using a cusp data base from the Polar satellite, limited to only events observed during southward IMF conditions [*Trattner et al.,* 2007]. To validate the prediction model, several studies used successfully observations of accelerated ion beams and ion beams that switched directions, while the observing satellite is in the magnetosheath boundary layer [e.g., *Fuselier et al.*, 2011; *Dunlop et al.,* 2011; *Trattner et al.,* 2012]. The Double Star magnetopause data base used in this study was also compared with the predictions form the Maximum Magnetic Shear model with an 84% success rate. However, 7 out of the 33 Double Star events occur during northward IMF conditions for which the prediction model also determined a maximum magnetic shear line

crossing the dayside magnetopause. In all seven cases the predicted reconnection location matched the confirmed reconnection location from Double Star TC1.

One of the seven northward IMF magnetopause events also had a fortunate conjunction with the Polar satellite located in the Southern Hemisphere cusp region. For this event we used the low-velocity cutoff methodology [e.g., *Onsager et al.,* 1990] used in the original Polar cusp study that led to the development of the Maximum Magnetic Shear model. Cutoff velocities for the incident and reflected ion beams in the cusp are used to calculate the distance to the reconnection site which is subsequently traced back along geomagnetic field lines from the cusp satellite location to the magnetopause [e.g., *Trattner et al.,* 2007]. These magnetopause trace points show the reconnection region where the cusp particles were injected onto newly opened field lines and also agree with the predicted line of maximum magnetic shear and the confirmed reconnection location from the Double Star TC1 magnetopause crossing.

This study expands the range of use of the Maximum Magnetic Shear model to include cases where reconnection occurs during northward IMF conditions (at least when B_Y is dominant). The applicability of the Maximum Magnetic Shear model for events with northward IMF conditions has also been reported in a comparative analysis of various reconnection models using global magnetosphere simulations [*Komar et al.,* 2015]. However, the exact IMF clock angle range for which dayside reconnection is possible, while the IMF has a positive B_z component still needs to be better understood. The lowest local magnetic shear in this study was about 50°, in agreement with earlier observations by *Gosling et al.* [1990]. A subsequent survey of the Polar cusp data base revealed that 29% of all cusp crossings under northward IMF conditions showed the typical cusp dispersion signature for a dayside reconnection line.

Acknowledgments
Solar wind observations were provided by the Wind "Solar Wind Experiment" (Wind/SWE) and by the ACE Solar Wind Experiment (ACE/SWE). The IMF measurements are provided by the Wind "Magnetic Field Instrument" (Wind/MFI) and by the ACE Magnetic Field Instrument (ACE/MFI). The solar wind data are available at CDAWeb (http://cdaweb.gsfc.nasa.gov/istp_public/). The research at LASP is also supported by a NASA grant NNX11AJ09G and NNX14AF71G and by the NSF under grant 1102572. Research at SWRI was funded by NASA grant NNX11AF71G. Research at Lockheed Martin was funded by NSF grant 1303186 and NASA grant 1415GC0062. The authors thank the International Space Science Institute in Bern, Switzerland, its staff, and directors for supporting the ISSI team "From Cluster to MMS," from which this work was partly developed.

References

Burch, J. L., P. H. Reiff, R. A. Heelis, J. D. Winningham, W. B. Hanson, C. Gurgiolo, J. D. Menietti, R. A. Hoffman, and J. N. Barfield (1982), Plasma injection and transport in the mid-altitude polar cusp, *Geophys. Res. Lett.*, *9*, 921–924, doi:10.1029/GL009i009p00921.

Burch, J. L., T. E. Moore, R. B. Torbert, and B. L. Giles (2016), Magnetospheric multiscale overview and science objectives, *Space Sci. Rev.*, *199*, 5–21, doi:10.1007/s11214-015-0164-9.

Carr, C., et al. (2005), The Double Star magnetic field investigation: Instrument design, performance and highlights of the first years of observations, *Ann. Geophys.*, *23*, 2713–2732, doi:10.5194/angeo-23-2713-2005.

Chandler, M. O., S. A. Fuselier, M. Lockwood, and T. E. Moore (1999), Evidence of component merging equatorward of the cusp, *J. Geophys. Res.*, *104*, 22,623–22,633, doi:10.1029/1999JA900175.

Cooling, B. M. A., C. J. Owen, and S. J. Schwartz (2001), Role of the magnetosheath flow in determining the motion of open flux tubes, *J. Geophys. Res.*, *106*, 18,763–18,775.

Cowley, S. W. H. (1982), The cause of convection in the Earth's Magnetosphere: A review of developments during the IMS, *Rev. Geophys. Res.*, *20*, 531–565, doi:10.1029/RG020i003p00531.

Cowley, S. W. H., and C. J. Owen (1989), A simple illustrative model of open flux tube motion over the dayside magnetopause, *Planet. Space Sci.*, *37*, 1461–1475, doi:10.1016/0032-0633(89)90116-5.

Cowley, S. W. H., M. P. Freeman, M. Lockwood, and M. F. Smith (1991), The ionospheric signature of flux transfer events, in *Cluster: Dayside Polar Cusp, ESA SP-330*, pp. 105–112 , ESA, Noordwijk, Neth.

Crooker, N. U. (1979), Dayside merging and cusp geometry, *J. Geophys. Res.*, *84*, 951–959, doi:10.1029/JA084iA03p00951.

Dungey, J. W. (1961), Interplanetary magnetic field and auroral zones, *Phys. Rev. Lett.*, *6*, 47–48, doi:10.1103/PhysRevLett.6.47.

Dungey, J. W. (1963), The structure of the ionosphere, or adventures in velocity space, in *Geophysics: The Earth's Environment*, edited by C. DeWitt, J. Hiebolt, and A. Lebeau, pp. 526–536, Gordon and Breach, New York.

Dunlop, M. W., Q.-H. Zhang, C.-J. Xiao, Z. Pu, R. Fear, C. Shen, and C. P. Escoubet (2009), Reconnection at high latitudes: Dayside anti-parallel merging, *Phys. Rev. Lett.*, *102*, 075005, doi:10.1103/PhysRevLett.102.075005.

Dunlop, M. W., et al. (2011), Magnetopause reconnection across wide local time, *Ann. Geophys.*, *29*, 1683–1697, doi:10.5194/angeo-29-1683-2011.

Escoubet, C. P., M. F. Smith, S. F. Fung, P. C. Anderson, R. A. Hoffman, E. M. Baasinska, and J. M. Bosqued (1992), Staircase ion signature in the polar cusp: A case study, *Geophys. Res. Lett.*, *19*, 1735–1738, doi:10.1029/92GL01806.

Escoubet, C. P., et al. (2006), Temporal evolution of a staircase ion signature observed by Cluster in the mid-altitude polar cusp, *Geophys. Res. Lett.*, *33*, L07108, doi:10.1029/2005GL025598.

Escoubet, C. P., et al. (2007), Two sources of magnetosheath ions observed by Cluster in the mid-altitude polar cusp, *Adv. Space Res.*, doi:10.1016/jasr.2007.04.031.

Escoubet C. P., et al. (2008), Effect of the IMF northward turning on the cusp precipitation as observed by Cluster, *J. Geophys. Res.*, *113*, A07S13, doi:10.1029/2007JA012771.

Escoubet, C. P., et al. (2013), Double cusp encounter by cluster: Double cusp or motion on the cusp?, *Ann. Geophys.*, *31*, 713–723, doi:10.5194/angeo-31-713-2013.

Frey, H. U., T. D. Phan, S. A. Fuselier, and S. B. Mende (2003), Continuous magnetic reconnection at Earth's magnetopause, *Nature*, *426*, 533–537, doi:10.1038/nature02084.

Fuselier, S. A., D. M. Klumpar, and E. G. Shelley (1991), Ion reflection and transmissions during reconnection at the Earth's subsolar magnetopause, *Geophys. Res. Lett.*, *18*, 139–142, doi:10.1029/90GL02676.

Fuselier, S. A., B. J. Anderson, and T. G. Onsager (1997), Electron and ion signatures of field line topology at the low-shear magnetopause, *J. Geophys. Res.*, *102*, 4847–4863, doi:10.1029/96JA03635.

Fuselier, S. A., S. M. Petrinec, and K. J. Trattner (2000), Stability of the high-latitude reconnection site for steady northward IMF, *Geophys. Res. Lett.*, *27*, 473–476, doi:10.1029/1999GL003706.

Fuselier, S. A., H. U. Frey, K. J. Trattner, S. B. Mende, and J. L. Burch (2002), Cusp aurora dependence on interplanetary magnetic field B_z, *J. Geophys. Res.*, *107*(A7), 1111, doi:10.1029/2001JA900165.

Fuselier, S. A., S. B. Mende, T. E. Moore, H. U. Frey, S. M. Petrinec, E. S. Claflin, and M. R. Collier (2003), Cusp dynamics and ionospheric outflow, *Space Sci. Rev.*, *109*, 285–312, doi:10.1023/B:SPAC.0000007522.71147.b3.

Fuselier, S. A., K. J. Trattner, and S. M. Petrinec (2011), Antiparallel and component reconnection at the dayside magnetopause, *J. Geophys. Res.*, *116*, A10227, doi:10.1029/2011JA016888.

Gonzalez, W. D., and F. S. Mozer (1974), A quantitative model for the potential resulting from reconnection with an arbitrary interplanetary magnetic field, *J. Geophys. Res.*, *79*, 4186–4194, doi:10.1029/JA079i028p04186.

Gosling, J. T., J. R. Asbridge, S. J. Bame, W. C. Feldman, G. Paschmann, N. Sckopke, and C. T. Russell (1982), Evidence for quasi stationary reconnection at the dayside magnetopause, *J. Geophys. Res.*, *87*, 2147–2158, doi:10.1029/JA087iA04p02147.

Gosling, J. T., M. F. Thomsen, S. J. Bame, R. C. Elphic, and C. T. Russell (1990), Cold ion beams in low-latitude boundary layer during accelerated flow events, *Geophys. Res. Lett.*, *17*, 2245–2248, doi:10.1029/GL017i012p02245.

Gosling, J. T., M. F. Thomsen, S. J. Bame, R. C. Elphic, and C. T. Russell (1991), Observations of reconnection of interplanetary and lobe magnetic field lines at the high-latitude magnetopause, *J. Geophys. Res.*, *96*, 14,097–14,106, doi:10.1029/91JA01139.

Kessel, R. L., S.-H. Chen, J. L. Green, S. F. Fung, S. A. Boarden, L. C. Tan, T. E. Eastman, J. D. Craven, and L. A. Frank (1996), Evidence of high latitude reconnecting during northward IMF: Hawkeye observations, *Geophys. Res. Lett.*, *23*, 583–586, doi:10.1029/95GL03083.

Kobel, E., and E. O. Flückiger (1994), A model of the steady state magnetic field in the magnetosheath, *J. Geophys. Res.*, *99*, 23,617–23,622, doi:10.1029/94JA01778.

Komar, C. M., R. L. Fermo, and P. A. Cassak (2015), Comparative analysis of dayside magnetic reconnection models in global magnetosphere simulations, *J. Geophys. Res. Space Physics*, *120*, 276–294, doi:10.1002/2014JA020587.

Lavraud, B., et al. (2005), Cluster observes the high-altitude cusp region, *Surv. Geophys.*, *26*(1–3), 135–175, doi:10.1007/s10712-005-1875-3.

Lepping, R. P., et al. (1995), The Wind Magnetic Field Instrument, in *The Global Geospace Mission*, edited by C. T. Russell, pp. 207–227, Kluwer Acad. Press, Netherlands.

Liu, Z. X., C. P. Escoubet, Z. Pu, H. Laakso, J. K. Shi, C. Shen, and M. Hapgood (2005), The Double Star mission, *Ann. Geophys.*, *23*, 2707–2712, doi:10.5194/angeo-23-2707-2005.

Lockwood, M., and M. F. Smith (1989), Low-altitude signatures of the cusp and flux transfer events, *Geophys. Res. Lett.*, *16*, 879–882.

Lockwood, M., and M. F. Smith (1992), The variation of reconnection rate at the dayside magnetopause and cusp ion precipitation, *J. Geophys. Res.*, *97*, 14,841–14,847, doi:10.1029/92JA01261.

Lockwood, M., and M. F. Smith (1994), Low- and mid-altitude cusp particle signatures for general magnetopause reconnection rate variations, I Theory, *J. Geophys. Res.*, *99*, 8531–8555.

Luhmann, J. R., R. J. Walker, C. T. Russell, N. U. Crooker, J. R. Spreiter, and S. S. Stahara (1984), Patterns of potential magnetic field merging sites on the dayside magnetopause, *J. Geophys. Res.*, *89*, 1739–1742, doi:10.1029/JA089iA03p01739.

McComas, D. J., S. J. Bame, P. Barker, W. C. Feldman, J. L. Phillips, P. Riley, and J. W. Griffee (1998), Solar Wind Electron Proton Alpha Monitor (SWEPAM) for the Advanced Composition Explorer, *Space Sci. Rev.*, *86*, 563–612, doi:10.1023/A:1005040232597.

Moore, T. E., M.-C. Fok, and M. O. Chandler (2002), The dayside reconnection X line, *J. Geophys. Res.*, *107*(A10), 1332, doi:10.1029/2002JA009381.

Newell, P. T., and C.-I. Meng (1991), Ion acceleration at the equatorward edge of the cusp: Low-altitude observations of patchy merging, *Geophys. Res. Lett.*, *18*, 1829–1832, doi:10.1029/91GL02088.

Ogilvie, K. W., et al. (1995), SWE: A comprehensive plasma instrument for the Wind spacecraft, in *The Global Geospace Mission*, edited by C. T. Russell, pp. 55–77, Kluwer Acad. Press, Norwell, Mass.

Oieroset, M., P. E. Sandholt, W. F. Denig, and S. W. H. Cowley (1997), Northward interplanetary magnetic field cusp aurora and high latitude magnetopause reconnection, *J. Geophys. Res.*, *102*, 11,349–11,362, doi:10.1029/97JA00559.

Onsager, T. G., and S. A. Fuselier (1994), The location of magnetic reconnection for northward and southward interplanetary magnetic field, in *Solar System Plasmas in Space and Time*, *Geophys. Monogr. Ser.*, vol. 84, edited by J. L. Burch and J. H. Waite Jr., pp. 183, AGU, Washington, D. C.

Onsager, T. G., M. F. Thomsen, J. T. Gosling, and S. J. Bame (1990), Electron distributions in the plasma sheet boundary layer: Time-of-flight effects, *Geophys. Res. Lett.*, *17*, 1837–1840, doi:10.1029/GL017i011p01837.

Onsager, T. G., M. F. Thomsen, R. C. Elphic, and J. T. Gosling (1991), Model of electron and ion distributions in the plasma sheet boundary layer, *J. Geophys. Res.*, *96*, 20,999–21,011, doi:10.1029/91JA01983.

Onsager, T. G., J. D. Scudder, M. Lockwood, and C. T. Russell (2001), Reconnection at the high-latitude magnetopause during northward interplanetary magnetic field conditions, *J. Geophys. Res.*, *106*, 25,467–25,488, doi:10.1029/2000JA000444.

Paschmann, G., B. U. Ö. Sonnerup, I. Papamastorakis, N. Sckopke, G. Haerendel, S. J. Bame, J. R. Asbridge, J. T. Gosling, J. T. Russell, and R. C. Elphic (1979), Plasma Acceleration at the Earth's magnetopause: Evidence for magnetic field reconnection, *Nature*, *282*, 243–246, doi:10.1038/282243a0.

Petrinec, S. M., K. J. Trattner, S. A. Fuselier, and J. Stovall (2014), The steepness of the magnetic shear angle 'saddle': A parameter for constraining the location of dayside magnetic reconnection?, *J. Geophys. Res. Space Physics*, *119*, 8404–8414, doi:10.1002/2014JA020209.

Petrinec, S. M., et al. (2016), Comparison of Magnetospheric Multiscale ion jet signatures with predicted reconnection site locations at the magnetopause, *Geophys. Res. Lett.*, *42*, 5997–6004, doi:10.1002/2016GL069626.

Phan, T. D., et al. (2003), Simultaneous Cluster and IMAGE Observations of cusp reconnection and auroral proton spot for northward IMF, *Geophys. Res. Lett.*, *30*(10), 1509, doi:10.1029/2003GL016885.

Phan, T. D., et al. (2004), Cluster observations of continuous reconnection at the magnetopause under steady interplanetary magnetic field conditions, *Ann. Geophys.*, *22*(7), 2355–2367, doi:10.5194/angeo-22-2355-2004.

Phan, T. D., et al. (2006), A magnetic reconnection X-line extending more than 390 Earth radii in the solar wind, *Nature*, *439*, 175–178, doi:10.1038/nature04393.

Phan, T.-D., G. Paschmann, and B. U. Ö. Sonnerup (1996), Low latitude dayside magnetopause and boundary layer for high magnetic shear 2. Occurrence of magnetic reconnection, *J. Geophys. Res.*, *101*, 7817–7828, doi:10.1029/95JA03751.

Phan, T.-D., et al. (2000), Extended magnetic reconnection at the Earth's magnetopause from detection of bi-directional jets, *Nature*, *404*, 848–850, doi:10.1038/35009050.

Pitout, F., C. P. Escoubet, B. Klecker, and I. Dandouras (2009), Cluster survey of the mid-altitude cusp—Part 2: Large-scale Morphology, *Ann. Geophys.*, *27*, 1875–1886.

Pu, Z.-Y., et al. (2007), Global view of dayside magnetic reconnection with the dawn-dusk IMF orientation: A statistic study for TC-1 and Cluster data, *Geophys. Res. Lett.*, *34*, L20101, doi:10.1029/2007GL030336.

Reme, H., et al. (2005), The HIA instrument on board the Tan Ce 1 Double Star near-equatorial spacecraft and its first results, *Ann. Geophys.*, *23*, 2757–2774, doi:10.5194/angeo-23-2757-2005.

Rosenbauer, H., H. Grünwaldt, M. D. Montgomery, G. Paschmann, and N. Sckopke (1975), Heos 2 plasma observations in the distant polar magnetosphere: The plasma mantle, *J. Geophys. Res.*, *80*, 2723–2737.

Sandholt, P. E., C. J. Farrugia, J. Moen, O. Noraberg, B. Lybekk, T. Sten, and T. L. Hansen (1998), A classification of dayside auroral forms and activities as a function of IMF orientation, *J. Geophys. Res.*, *103*, 23,325–23,345, doi:10.1029/98JA02156.

Shelley, E. G., R. D. Sharp, and R. G. Johnson (1976), He++ and H+ flux measurements in the day side cusp: Estimates of convection electric field, *J. Geophys. Res.*, *81*, 2363–2370.

Shelley, E. G., et al. (1995), The Toroidal Imaging Mass-Angle Spectrograph (TIMAS) for the Polar mission, *Space Sci. Rev.*, *71*, 497–530, doi:10.1007/BF00751339.

Sibeck, D. G., R. E. Lopez, and E. C. Roelof (1991), Solar wind control of the magnetopause shape, location, and motion, *J. Geophys. Res.*, *96*, 5489–5495, doi:10.1029/90JA02464.

Smith, C. W., M. H. Acuna, L. F. Burlaga, J. L. Heureux, N. F. Ness, and J. Scheifele (1998), The ACE Magnetic Field Experiment, *Space Sci. Rev.*, *86*, 613, doi:10.1023/A:1005092216668.

Smith, E. J., and M. Lockwood (1990), The pulsating cusp, *Geophys. Res. Lett.*, *17*, 1068–1072, doi:10.1029/GL017i008p01069.

Sonnerup, B. U. Ö. (1974), The reconnecting magnetosphere, in *Magnetospheric Physics, Proceedings of the Advanced Summer Institute, held at Sheffield, UK, 1973*, *Astrophys. Space Science Library*, vol. 44, edited by B. M. McCormas, pp. 23, D. Reidel, Dortrecht.

Sonnerup, B. U. Ö., G. Paschmann, I. Papamastorakis, N. Sckopke, G. Haerendel, S. J. Bame, J. R. Asbridge, J. T. Gosling, and C. T. Russell (1981), Evidence for magnetic field reconnection at the Earth's magnetopause, *J. Geophys. Res.*, *86*, 10,049–10,067, doi:10.1029/JA086iA12p10049.

Trattner, K. J., S. A. Fuselier, W. K. Peterson, and C. W. Carlson (2002), Spatial features observed in the cusp under steady solar wind conditions, *J. Geophys. Res.*, *107*(A10), 1288, 10.1029/2001JA000262.

Trattner, K. J., S. M. Petrinec, and S. A. Fuselier (2004), Location of the reconnection line for northward interplanetary magnetic field, *J. Geophys. Res.*, *109*, A03219, doi:10.1029/2003JA009975.

Trattner, K. J., J. S. Mulcock, S. M. Petrinec, and S. A. Fuselier (2007), Probing the boundary between anti-parallel and component reconnection during southwards interplanetary magnetic field conditions, *J. Geophys. Res.*, *112*, A08210, doi:10.1029/2007JA012270.

Trattner, K. J., S. M. Petrinec, S. A. Fuselier, and T. D. Phan (2012), The location of the reconnection line: Testing the Maximum Magnetic Shear model with THEMIS observations, *J. Geophys. Res.*, *117*, A01201, doi:10.1029/2011JA016959.

Trattner, K. J., et al. (2016), The response time of the magnetopause reconnection location to changes in the solar wind: MMS case study, *Geophys. Res. Letters*, *43*, 4673–4682, doi:10.1002/2016GL068554.

Trenchi, L., M. F. Marcucci, G. Pallocchia, G. Consolini, M. B. Bavassano Cattaneo, A. M. Di Lellis, H. Rème, L. Kistler, C. M. Carr, and J. B. Cao (2008), Occurrence of reconnection jets at the dayside magnetopause: Double Star observations, *J. Geophys. Res.*, *113*, A07S10, doi:10.1029/2007JA012774.

Trenchi, L., M. F. Marcucci, G. Pallocchia, G. Consolini, M. B. Cattaneo, A. Di Lellis, H. Rème, L. Kistler, C. M. Carr, and J. B. Cao (2009), Magnetic reconnection at the dayside magnetopause with Double Star TC1 data, *Mem. Soc. Astron. Ital.*, *80*, 287.

Trenchi, L., M. F. Marcucci, and R. C. Fear (2015), The effect of diamagnetic drift on motion of the dayside magnetopause reconnection line, *Geophys. Res. Letter*, *42*, 6129–6136, doi:10.1002/2015GL065213.

Tsyganenko, N. A. (1995), Modeling the Earth's magnetospheric magnetic field confined within a realistic magnetopause, *J. Geophys. Res.*, *100*, 5599–5612, doi:10.1029/94JA03193.

Vines, S. K., S. A. Fuselier, K. J. Trattner, S. M. Petrinec, and J. F. Drake (2015), Ion acceleration dependence on shear angle in dayside magnetopause reconnection, *J. Geophys. Res. Space Physics*, *120*, 7255–7269, doi:10.1002/2015JA021464.

Wing, S., P. T. Newell, and J. M. Rouhoniemi (2001), Double Cusp: Model prediction and observational verification, *J. Geophys. Res.*, *106*, 25,571–25,593, doi:10.1029/2000JA000402.